· Article · Advances in Polar Science
doi: 10.12429/j.advps.2025.0031 December 2025 Vol. 36 No. 4: 301-319

Discovery of new polyketide–amino acid conjugates in Antarctic-derived *Talaromyces* sp. HDN1820200 by overexpression of a pathway-specific transcriptional factor TwnD

ZHANG Xiao[1], LIU Luyang[1], MA Chuanteng[1], CHE Qian[1], LI Dehai[1,2,3] & ZHU Tianjiao[1,2,3*]

[1] Key Laboratory of Marine Drugs Ministry of Education, Ocean University of China, Qingdao 266003, China;
[2] Laboratory for Marine Drugs and Bioproducts, Qingdao Marine Science and Technology Center, Qingdao 266237, China;
[3] Sanya Oceanographic Institute, Ocean University of China, Sanya 572025, China

Received 21 September 2025; accepted 25 November 2025; published online 30 December 2025

Abstract A polyketide synthase–nonribosomal peptide synthetase gene cluster *twn* in *Talaromyces* sp. HDN1820200 was activated by overexpression of the pathway-specific transcriptional factor TwnD. Large-scale fermentation and chemical investigation of the mutant strain HDN1820200/TwnD led to the discovery of one new polyketide–amino acid conjugate, bipolamide C and one new polyketide compound, variotin A. The structures of the new compounds were determined by nuclear magnetic resonance (NMR) analysis, high-resolution electrospray ionization mass spectrometry, feeding experiments, NMR calculation and DP4$^+$ analysis. This study revealed that the overexpression of the pathway-specific transcriptional factor represents a promising approach for the discovery of new natural products in fungi within specialized habitat.

Keywords **transcription factor overexpression, polyketide–amino acid conjugates, Antarctic fungi, natural product discovery**

Citation: Zhang X, Liu L Y, Ma C T, et al. Discovery of new polyketide–amino acid conjugates in Antarctic-derived *Talaromyces* sp. HDN1820200 by overexpression of a pathway-specific transcriptional factor TwnD. Adv Polar Sci, 2025, 36(4): 301-319, doi: 10.12429/j.advps.2025.0031

1 Introduction

Antarctica, featured by its extreme environmental conditions, harbors a unique and largely untapped reservoir of biodiversity (Wauchope et al., 2019). Microorganisms thriving in this harsh ecosystem have evolved sophisticated metabolic pathways to survive under perpetual cold, desiccation, and nutrient scarcity, rendering them prolific sources of novel bioactive compounds (Shu et al., 2022). Among these, polyketide–amino acid (PKAA) conjugates represent a structurally diverse class of natural products with significant pharmaceutical potential, exemplified by their roles as antimicrobial (Kudo, 2024), anticancer (Gao et al., 2021), and immunomodulatory agents (Morán et al., 2004). PKAA conjugates are considered to play a role as signaling molecules that regulate many physiological processes. For example, *N*-arachidonoylglycine is both GPR18 (Grabiec et al., 2019) and GPR55 (Console-Bram et al., 2017) ligand that can act as an appropriate target for the development of anti-hypertensive or anti-hypotensive.

* Corresponding author. E-mail: zhutj@ouc.edu.cn

However, the PKAA conjugates from Antarctic-derived fungi remain underexplored, as many cryptic gene clusters are usually transcriptionally silent under standard laboratory conditions.

Recent advances in genome mining have revealed that extremophilic fungi, such as those from Antarctica, encode a wealth of silent biosynthetic gene clusters (BGCs), which are hypothesized to produce specialized metabolites under ecological stress (Scherlach and Hertweck, 2021). Activating these pathways is critical to unlocking their chemical diversity. Strategies such as the overexpression of pathway-specific transcriptional regulators and heterologous expression have emerged as powerful tools to activate the silent BGCs (Rutledge and Challis, 2015; Seshadri et al., 2025). This approach circumvents the limitations of traditional cultivation-based methods and aligns with the growing demand for innovative natural product discovery from underexplored habitats.

In this study, we focus on *Talaromyces* sp. HDN1820200, a fungus isolated from Antarctic sponge, which harbors a cryptic polyketide synthase–nonribosomal peptide synthetase (PKS-NRPS) gene cluster (*twn*). Bioinformatic analysis reveals that *twn* BGC may be responsible for the biosynthesis of an unknown PKAA conjugate. By overexpressing the cluster-specific Zn(II)Cys6 transcriptional factor TwnD, this silent BGC was successfully activated and its products had been elucidated. Detailed feeding and gene-disruption experiments show that the 4-*oxo*-isoleucine, a new amino acid derivative which is oxidated from *L*-Ile, is introduced into the bipolamide C.

2 Materials and methods

2.1 Instruments and solutions

The instruments and main reagents used in this experiment are described as follows: SW-CJ series clean bench (Suzhou Antai Air Technology Co., Ltd., Suzhou, China); CX41 biological microscope (Olympus Corporation, Tokyo, Japan); Neofuge 15R/13R high-speed refrigerated centrifuge (Shanghai Lishen Scientific Instrument Co., Ltd., Shanghai, China); vacuum centrifugal concentrator and freeze dryer (CIMO Inter-national Group, Jinximo (Beijing) Co., Ltd., Beijing, China); LDZX-75KB vertical pressure steam sterilizer (Shanghai Shenan Medical Equipment Factory, Shanghai, China); JA21002 electronic balance (Shanghai Jingtian Electronic Instrument Factory, Shanghai, China); SPX intelligent biochemical incubator (Ningbo Jiangnan Instrument Factory, Ningbo, China); Life Pro gene amplification instrument (Hangzhou Bioer Technology Co., Ltd., Hangzhou, China); SensiAnsys gel image analysis system (Shanghai Peiqing Technology Co., Ltd., Shanghai, China); EPS-600 electrophoresis apparatus (Shanghai Tianneng Technology Co., Ltd., Shanghai, China); HE-120 multifunctional horizontal electrophoresis tank (Shanghai Tianneng Technology Co., Ltd., Shanghai, China); gel recovery kit (Omega Bio-tek Inc., Norcross, USA); plasmid mini-prep kit (Tsingke Biotechnology Co., Ltd., Beijing, China); *Escherichia coli* super competent cell preparation kit (Beyotime Biotechnology Co., Ltd., Shanghai, China); Hieff Canace high-fidelity DNA polymerase (Shanghai Yisheng Biotechnology Co., Ltd., Shanghai, China); 2×Hieff PCR Master Mix (With Dye) (Shanghai Yisheng Bio-technology Co., Ltd., Shanghai, China); driselase (Shanghai Yuanye Biotechnology Co., Ltd., Shanghai, China); snailase (Shanghai Yuanye Biotechnology Co., Ltd., Shanghai, China); hygromycin (Solarbio Biotechnology Co., Ltd., Beijing, China); and ampicillin (Shanghai Sangon Biotech Co., Ltd. , Shanghai, China). PCR primer synthesis and sequencing were performed by Sangon Biotech (Qingdao) Co., Ltd. (Qingdao, China).

2.2 Materials and culture conditions

The fungal strain *Talaromyces* sp. HDN1820200 was isolated from the sponge sample. The strain was identified by an internal transcribed spacer sequence, and the sequence data were submitted to GenBank (GenBank accession no. MW031818). The strain was deposited at the Marine Medicinal Bioresources Center, Ocean University of China, China. For genomic DNA extraction, *Talaromyces* sp. HDN1820200 was cultured at 28 ℃ on PDA plates for 5 d. *E. coli* DH5α was used for plasmids preservation and amplification. *Saccharomyces cerevisiae* BJ5464-NpgA was used for in vivo DNA recombination for plasmids construction. The control strain and *OE::twnD* strain were cultured in PDB media at 28 ℃, 220 rpm for fermentation and compound production. *Talaromyces* sp. HDN1820200 was grown at 28 ℃ in PSA (PDA with 1.2 mol·L^{-1} D-sorbitol and 200 μg·mL^{-1} hygromycin) or in PSA (PDA with 1.2 mol·L^{-1} D-sorbitol and 200 μg·mL^{-1} G418) to screen transformants.

2.3 Sequence analysis of the *twn* BGC and *TwnA* gene

The *twn* BGC were analyzed by antiSMASH (Blin et al., 2023). The phylogenetic analysis was conducted with MEGA-X software (version 10.0.0) (Kumar et al., 2018) with the amino acid sequences of TwnA and reported C domains retrieved from the NCBI. The conserved domain of the TwnA protein was scanned by the InterProScan program (Quevillon et al., 2005). Comparative analysis between the *twn* BGC and *twm* BGC was conducted by Clinker (Gilchrist and Chooi, 2021).

2.4 Gene cloning, plasmid construction, and genetic manipulation

The strains, plasmids and the oligonucleotide sequences of the PCR primers utilized in this study are as follows. The Q5 High-Fidelity DNA polymerase and restriction endonuclease, indispensable for all DNA processing, were obtained from New England Biolabs

Corporation (Ipswich, USA). The Frozen-EZ Yeast Transformation II Kit (Zymo Research, Irvine, USA) and the Zymoprep Yeast Plasmid Miniprep I Kit (Zymo Research, Irvine, USA) were employed for yeast transformation and plasmid recombination. The expression plasmids were generated through yeast homologous recombination in *S. cerevisiae* BJ5464-NpgA. Plasmid pHyg was digested with *Kpn*I and *Xba*I, while plasmid pYEU was digested with *Nde* I and *Pml* I to serve as vectors for gene insertion (Figure S1). To construct plasmid pHyg-TwnD, TwnD was amplified by PCR using the primer pair TwnD-F/R and cloned into vector pHyg. Strains and plasmids used in this study were listed in Table 1.

To construct plasmid pYEU-KO-TwnB, the TwnB-upstream, G418 resistant gene and TwnB-downstream fragments were amplified using the primer pairs TwnB-upstream-F/R, G418-F/R, and TwnB-downstream-F/R, respectively and then cloned into vector pYEU. The construction of plasmid pYEU-KO-TwnA involved the amplification of TwnA-upstream, G418 resistant gene and TwnA-downstream fragments by PCR using the TwnA-upstream-F/R, G418-F/R, and TwnA-downstream-F/R primer pairs, respectively. Primers used in this study were shown in Table 2.

Table 1 Strains and plasmids used in this study

Strain/plasmid	Characteristics/use	Source
Talaromyces sp. HDN1820200	Isolated from Antarctic sponge sample	This study
Escherichia coli DH5α	Host bacteria for plasmid preservation and cloning	This study
Saccharomy cescerevisiae BJ5464-NpgA	Nutritionally deficient yeast strains (Ura-, Trp-, Leu-) as vectors with homologous recombination of gene fragments in host strains	This study
Ts-pHyg	Harboring empty pHyg vectors	This study
Ts-OE::TwnD	Harboring the plasmid pHyg-TwnD	This study
Ts-OE::TwnD-KO-TwnA	Harboring the plasmid pHyg-TwnD and knockout-TwnA	This study
Ts-OE::TwnD-KO-TwnB	Harboring the plasmid pHyg-TwnD and knockout-TwnB	This study
pHyg	Contains the hygromycin resistance gene as an overexpression vector plasmid with the gene fragment inserted after the promoter gpdA	This study
pG418	Contains the G418 resistant gene as an overexpression vector plasmid with the gene fragment inserted after the promoter gpdA	This study
pYEU	Containing the *Ura* gene as a vector plasmid	This study
pHyg-TwnD	*TwnD* gDNA with downstream 500 bp used the promoter gpdA in *Xba*I and *Kpn*I-linearized pHyg	This study
pYEU-KO-TwnA	*TalsA* upstream 1,500 bp, G418 resistant gene and TalsA downstream 1,500 bp in *Nde*I and *Pac*I-linearized pYEU	This study
pYEU-KO-TwnB	*TalsE* upstream 1,500 bp, G418 resistant gene and TalsB downstream 1,500 bp in *Nde*I and *Pac*I-linearized pYEU	This study

Table 2 The primers used in this study

Primer name	Sequences (5'→3')	Function
TwnD-F	ggcaggaccggacggggcggtaccCTCTCCTCCCACTCTAGTCTCTT	For *TwnD* fragment amplification and recombinant plasmid validation
TwnD-R	cgataccgtcgacctcgactctagaATGCAAACACCGGGTGTG	
OE::TwnD-yz-F	CGACAGATGTGAGAAGGCAGATG	For *OE::TwnD* transformants validation
OE::TwnD-yz-R	CATCTAGAAGTATCTTGCCTGTC	
TwnA-upstream-F	aaggatgatgatgataagactagtGTGCTTATCTGCGAGGGACCTTC	For *TwnA* upstream fragment amplification
TwnA-upstream-R	TGTAAGCGTTAATCTAGACATTTTGAATCGAGTTCTTGGT	
TwnA-downstream-F	AAGTTCCTATTCTCTAGAAAACCATGAAGGTTTTCGAAAT	For *TwnA* downstream fragment amplification
TwnA-downstream-R	gtgatggtgatggtgatgcacgtgAAGAAATCCGTTGCGGGCTC	
TwnB-upstream-F	aaggatgatgatgataagactagtCTGCTGGTTTTTCGCCGTGTTTC	For *TwnB* upstream fragment amplification
TwnB-upstream-R	TGTAAGCGTTAATCTAGACGCAAACAATCGTGTATCTTCC	
TwnB-downstream-F	AAGTTCCTATTCTCTAGAGCATGGATTCAGAAGCTCGAGG	For *TwnB* downstream fragment amplification
TwnB-downstream-R	gtgatggtgatggtgatgcacgtgAGAACTATACCGCCAGACCCTG	
G418-F	TCTAGATTAACGCTTACAATTTCC	For G418 fragment amplification
G418-R	TCTAGAGAATAGGAACTTCGGAATAG	
YZ-TwnA-U-F	TGCAGGTCAATATCCTACGTGC	For *OE::TwnD-KO-TwnA* transformants validation
YZ-TwnA-U-R	GGCCACAGTCGATGAATCCAG	
YZ-TwnA-D-F	CTATCGCCTTCTTGACGAGTTCT	
YZ-TwnA-D-R	GGCAAAGCAGCAATCGCTCTA	

continued

Primer name	Sequences (5'→3')	Function
YZ-TwnB-U-F	TCAGCTGAACAGGATTTATAGGCAC	For *OE::TwnD-KO-TwnB* transformants validation
YZ-TwnB-U-R	GGCCACAGTCGATGAATCCAG	
YZ-TwnB-D-F	CTATCGCCTTCTTGACGAGTTCT	
YZ-TwnB-D-R	AGTGATGAGTAGGACGTGATTCTC	

2.5 Construction and verification of *OE::TwnD* strain, *OE::TwnD-KO-TwnA* strain and *OE::TwnD-KO-TwnB* strain

The preparation and transformation of fungal protoplasts were carried out according to the method described by Yee and Tang (2022). Three fungal transformants, namely *OE::TwnD*, *OE::TwnD-KO-TwnA* and *OE::TwnD-KO-TwnB* were constructed using polyethylene glycol (PEG) -mediated protoplast transformation. The plasmid pHyg-TwnD, was introduced into *Talaromyces* sp. HDN1820200 to generate the *OE::TwnD* strain, which was selected by PSA plates with hygromycin and subsequent confirmation by PCR amplification. The obtained constructs, pYEU-KO-TwnD and pYEU-KO-TwnA, were introduced into the *OE::TwnD* strain. Following G418 selection on PSA plates and PCR confirmation, integration transformants, *OE::TwnD-KO-TwnA* and *OE::TwnD-KO- TwnE* were obtained. Transformations with the empty vectors pHyg, or pG418 were performed as controls in PCR validation. The correct transformants were verified by PCR (Figures S2 and S3).

2.6 Fermentation and HPLC/LC-MS analyses

The obtained transformants were cultured on PDB medium and incubated at 28 ℃ for 9 d. Subsequently, the cultures were extracted for 3 times with ethyl acetate (EtOAc). The organic phase was evaporated to dryness using a rotary evaporator and redissolved in 300 μL of methanol (MeOH). Then, 50 μL of the dissolved extract was subjected to high-performance liquid chromatography–photodiode array detection–mass spectrometry (HPLC-DAD-MS) analysis (C18 column, Shimadzu, Kyoto, Japan; 4.6 mm×150 mm, 5 μm, 1 mL·min^{-1}). The samples were separated using a linear gradient of 15%–50% CH_3CN (MeCN) in water (0.1% trifluoroacetic acid) over 25 min at a flow rate of 1 mL·min^{-1}, followed by a linear gradient of 50%–100% MeCN in water (0.1% trifluoroacetic acid) for 10 min, and finally isocratic elution with 100% MeCN for 5 min. For HPLC analysis (C18 column, Shimadzu, Kyoto, Japan; 4.6 mm×150 mm, 5 μm, 1 mL·min^{-1}), the samples were first separated isocratically with 5% MeOH for 5 min at a flow rate of 1 mL·min^{-1}, followed by a linear gradient of 5%–100% MeOH in water (0.1% trifluoroacetic acid) over 30 min at a flow rate of 1 mL·min^{-1}, and finally isocratic elution with 100% MeOH for 5 min.

2.7 Extraction, isolation, and purification

The transformant *OE::TwnD* strain was subjected to large-scale cultivation in 15 L of PDB medium and incubated at 28 ℃ for 9 d. The medium obtained from the large-scale fermentation was extracted with EtOAc for 3 times, yielding a crude extract (6 g). The crude extract was then fractionated using an ODS reverse-phase column with a gradient elution of MeOH/H_2O, resulting in 10 fractions (Fr.1–Fr.10, 10%–100%). Fr.7 was further purified on a preparative C18 HPLC column using an isocratic elution of MeCN/H_2O (55:45), yielding compound **2** (3.5 mg). Fr.8 was purified on a preparative C18 HPLC column with an isocratic elution of MeOH/H_2O (75:35), yielding compound **1** (3.2 mg).

Bipolamide C (**1**): yellow amorphous solid powder; UV (MeOH) λ_{max} (log ε): 223 (0.4), 305 (0.8) nm, ^{1}H and ^{13}C NMR data in Table 3; HRESIMS *m/z* 320.1861 $[M-H]^-$ (calculated for $C_{18}H_{26}O_4N$ 320.1867).

Table 3 ^{1}H (400 MHz) and ^{13}C (100 MHz) NMR data of compounds **1** and **2** (DMSO-d_6)

No.	Compound **1**		No.	Compound **2**	
	δ_C	δ_H (*J*)/Hz		δ_C	δ_H (*J*)/Hz
1	172.2, C	-	1	168.1, C	-
2	53.3, CH	4.72, m	2	122.4, CH	5.91, d (15.08)
3	48.0, CH	2.97, m	3	138.5, CH	7.61, ddd (15.08, 11.46, 5.92)
4	208.3, C	-	4	125.5, CH	6.14, t (11.46)
5	28.2, CH_3	2.16, s	5	136.7, CH	6.37, t (11.46)
6	12.3, CH_3	1.04, d (6.95)	6	122.3, CH	6.76, dd (15.04, 11.46)
7-NH	-	8.13, d (6.95)	7	144.7, CH	6.00, dd (15.04, 6.59)
8	165.4, C	-	8	66.1, CH	4.27, d (6.59)
9	120.0, CH	6.21, d (15.35)	9	23.5, CH_3	1.15, m

continued

No.	Compound **1**		No.	Compound **2**	
	δ_C	δ_H (*J*)/Hz		δ_C	δ_H (*J*)/Hz
10	144.1, CH	7.08, d (15.35)	8-OH	-	4.92, d (4.51)
11	131.5, C	-			
12	137.0, CH	6.40, m			
13	125.1, CH	6.41, d (11.10)			
14	144.8, CH	5.83, m			
15	38.4, CH	2.20, m			
16	29.1, CH_2	1.33, dt (13.60, 7.15)			
17	11.7, CH_3	0.83, t (7.15)			
18	19.9, CH_3	0.99, d (6.80)			
19	12.5, CH_3	1.83, s			

Variotin A (**2**): yellow amorphous solid powder; UV (MeOH) λ_{max} (log ε): 223 (0.3), 305 (0.7) nm, ^{1}H and ^{13}C NMR data in Table 3; HRESIMS *m/z* 167.0718 $[M-H]^-$ (calculated for $C_9H_{11}O_3$ 167.0714).

3 Results

3.1 Bioinformatic analysis of the *twnA* and *twn* BGC in *Talaromyces* sp. HDN1820200

The backbone of PKAA conjugates is usually assembled by PKS-NRPS hybrid megasynthetase. Using TwmB (Hai et al., 2018), a fungal PKS-NRPS from the wortmanamide (a fungal PKAA conjugate) biosynthetic pathway, as a query protein, we searched for the potential PKAA conjugate BGCs in *Talaromyces* sp. HDN1820200 genome. A candidate cluster, named the *twn* cluster, that shared high similarity with *twm* cluster has been identified (Figure 1 and Table S1). The *twn* cluster encodes a PKS-NRPS (TwnA) and a P450 mono-oxygenase (TwnB), an MFS (TwnC), a Zn(II)Cys(6) transcriptional factor (TwnD), and a trans-enoyl reductase (TwnE) (Figure 1). Detailed analysis revealed that TwnA consists of 10 domains with a C-terminal putative reductive function R domain, while TwmB consists of 8 domains with a truncated condensation domain. Analysis of the active sites of TwnA-C domain showed that the TwnA-C domain contains a unique characteristic "HSXXXD" motif instead of the classical C domain "HHXXXD" motif (Keating et al., 2002). It has been proved in ThnB-CT that its second His residue is essential for condensation activity (Zhang et al., 2020), so the unique serine in TwnA-C domain may represent a novel catalytic function of fungal NRPS C domain in natural product biosynthesis. In addition, the results of phylogenetic tree analysis of the TwnA-C domain suggested that it is clustered with PKS-NRPS C domain which is responsible for PKAA synthesis (Figure 2).

3.2 Overexpression of TwnD to activate the *twn* BGC

To investigate the product of the *twn* cluster, the twnD gene with its own terminal was cloned from the gDNA of strain HDN1820200 under the gpdA constitutive promoter on pHyg plasmid and transformed into *Talaromyces* sp. HDN1820200 by PEG-mediated transformation (Liu and Friesen, 2012). Metabolite analysis showed that a series of peaks were detected in the *OE::TwnD* EtOAc extract compared to that of the control strain containing the empty vector (Figures 3 and S4). They all shared similar UV spectra with absorption maxima at 223 and 305 nm, indicating similar structures. However, due to the instability of these compounds, two compounds (**1** and **2**) were successfully isolated and identified.

3.3 Structure elucidation of compounds 1 and 2

Compound **1** was obtained as a yellow amorphous solid powder, and its molecular formula was established as $C_{18}H_{27}O_4N$ based on negative HRESIMS data, which

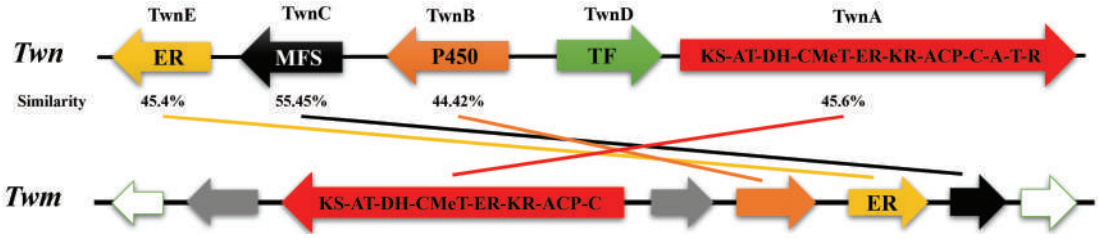

Figure 1 Comparison of the *twn* BGC from *Talaromyces* sp. HDN1820200 to *twm* BGC from *Talaromyces wortmannii* CBS 387.67.

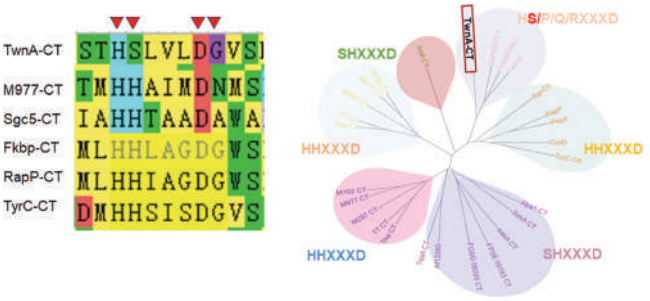

Figure 2 Sequence alignment and phylogenetic analysis of the condensation (C) domain from TwnA, showing its clustering with known polyketide-amino acid (PKAA) synthetases and its unique "HSXXXD" active site motif.

displayed a peak at *m/z* 320.1861 (calculated for $C_{18}H_{26}O_4N$, $[M-H]^-$, 320.1867) (Figure S5). According to the ^{1}H-NMR, ^{13}C-NMR data, **1** has five methyl carbons, one methylene carbon, eight tertiary carbons and four quaternary carbons (Figures S6, S7). The NMR data featured a PKAA derivative, which was structurally related to bipolamide A. In the ^{1}H-^{1}H COSY spectra, the correlations between H-2 (δ_H 4.72)/N-H (δ_H 8.13), H-2/H-3 (δ_H 2.97)/H-6 (δ_H 12.3), combined with the HMBC correlations between H-2 with C-1 (δ_C 172.2) and C-4 (δ_C 208.3), H-3 with C-4 and C-1, and H-5 (δ_H 2.16) with C-4 and C-3, determine the planar structure of the 4-*oxo*-isoleucine moity (Figures S8 and S9). Based on the ^{1}H-^{1}H COSY, the correlation of H-9 (δ_H 6.21)/H-10 (δ_H 7.08) and the HMBC correlations of H-9 with C-8 and C-11 (δ_C 131.5), H-10 (δ_H 7.08) with C-12 (δ_C 137.0) and C-19 (δ_C 12.5), H-12 (δ_H 6.40) with C-13 (δ_C 125.1), H-14 (δ_H 5.83) with C-15, C-16 (δ_C 29.1) and C-18 (δ_C 19.9), and H-16 (δ_H 1.33) with C-17 (δ_C 11.7), the polyketide planar structure was determined. The ^{1}H-^{1}H COSY spectrum further secured the proton connectivity within the polyketide chain. Key correlations were observed between H-13 (δ_H 6.41) and H-14, H-14 and H-15 (δ_H 2.20), and from H-15 to the methylene protons H-16 (δ_H 1.33), which in turn correlated with the terminal methyl group H-17 (δ_H 0.83). This continuous spin system, in conjunction with the HMBC data, unequivocally established the planar structure of the polyene moiety in compound **1** (Figures S10 and S11). The polyketide and the 4-*oxo*-isoleucine are connected via the carbonyl carbon at the C-8 position to the amino amide bond at the N-7 position, which can be determined by the HMBC correlation between H-2 and C-8. Accordingly, the planar structure of compound **1** is determined and was given the trivial name bipolamide C (Figure 4).

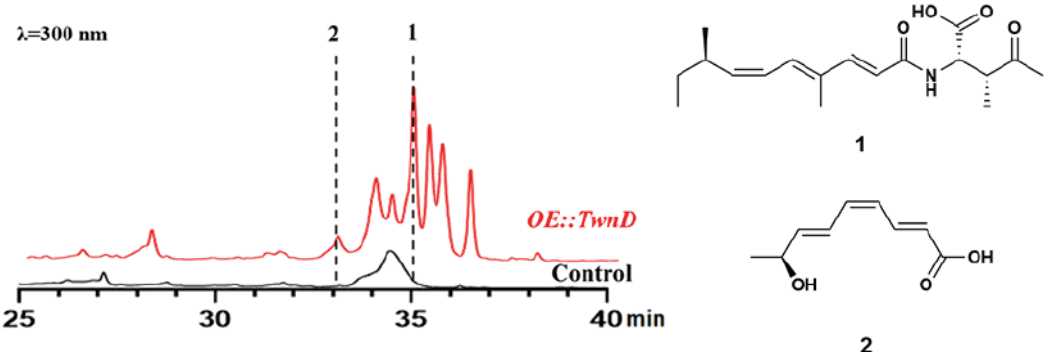

Figure 3 HPLC analysis (λ=300 nm) of ethyl acetate extracts from the *OE::TwnD* overexpression strain and the control strain. The structures of the newly isolated compounds **1** (bipolamide C) and **2** (variotin A) are shown.

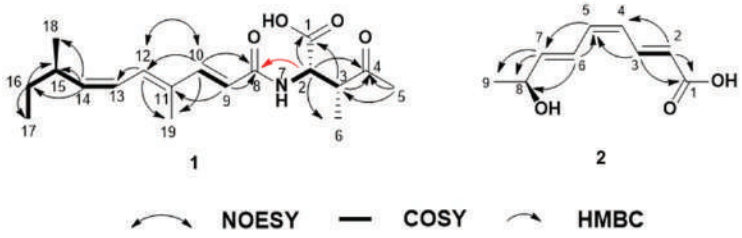

Figure 4 Key 2D NMR correlations of compounds **1** and **2**.

The configurations of the double bonds $\Delta_{9,10}$ and $\Delta_{13,14}$ were determined to be *E*-type and *Z*-type, respectively, on the basis of the $J_{H9\text{-}10}$ (J=15.35 Hz), and $J_{H13\text{-}14}$ (J=11.0 Hz) along with the NOESY correlation between H-13 and H-9. The NOESY correlation between H-10 and H-12 indicated that the configuration of the double bond $\Delta_{11,12}$ was *E*-type. The calculations of ^{13}C NMR chemical shifts of (*2S*, *3R*, *15S**), (*2S**, *3R**, *15R**), (*2S**, *3S**, *15S**), and (*2R**, *3S**, *15S**) of compound **1** at the B3LYP/6-311G (d,p) level in DMSO were finally carried out. The absolute configuration

of compound **1** was determined to be (*2S*, *3R*, *15R*) based on DP4$^+$ calculation (Text S1, Figure S12).

Compound **2** was obtained as a yellow amorphous solid powder, and its molecular formula was established as $C_9H_{12}O_3$ based on negative HRESIMS data, which displayed a peak at *m/z* 167.0718 (calculated for $C_9H_{11}O_3$, $[M-H]^-$, 167.0714) (Figure S13). According to the ^{1}H-NMR, ^{13}C-NMR data, **2** has one methyl carbon, seven methylene carbons, and one quaternary carbon (Figures S14 and S15). Based on the correlation of H-2 (δ_H 5.91)/H-3 (δ_H 7.61) in the ^{1}H-^{1}H COSY spectra, combined with the HMBC correlation of H-2 (δ_H 5.91) with C-1 (δ_C 168.1) and C-4 (δ_C 125.5), H-3 (δ_H 7.61) with C-1 and C-5, H-5 (δ_H 6.37) with C-7 (δ_C 6.37), H-6 (δ_H 6.76) with C-5 and C-8 (δ_C 66.1), and H-7 (δ_H 6.00) with C-8 and C-9, in combination with molecular weight and chemical shifts, the planar structure of compound **2** was determined and was given the trivial name variotin A (Figures S16–S18).

The J_{H2-3} (J=15.08 Hz), J_{H4-5} (J=11.46 Hz), and J_{H6-7} (J=15.04 Hz) determined the configurations of the double bonds $\Delta_{2,3}$, $\Delta_{4,5}$, and $\Delta_{6,7}$ to be the *E*-type, *Z*-type, and *E*-type, respectively. Compound **2** at the MPW1PW91/6-311G (d,p) level with the PCM in DMSO were finally carried out. The calculations of ^{13}C NMR chemical shifts of *8R** and *8S** of compound **2** at the B3LYP/6-311G (d,p) level in DMSO were carried out. The NMR calculation of compound **2** determined the absolute conformation of the C-8 position was *8S* (Figure S19).

3.4 Feeding experiment to determine that 4-*oxo*-isoleucine is originated from *L*-Ile

PKAA containing an amino acid derivative instead of an amino acid usually generated from amino acid oxidation. For example, 4-hydroxyproline in burnettramic acid A is generated from the hydroxylation of proline catalyzed by BuaE (Li et al., 2019). The bipolamide C was the first reported PKAA which has a 4-*oxo*-isoleucine substituted. Bipolamides A and B, triene amides isolated from the endophytic fungus *Bipolaris* sp. MU34 have similar 2-hydroxyl-4-*oxo*-isoleucine substituted (Siriwach et al., 2014). However, the biosynthetic origin of 4-*oxo*-isoleucine has never been investigated. We speculated that it was a product of the oxidation progress from isoleucine. To test this hypothesis, the *OE::TwnD* strain was pre-cultured for 3 d. Then different amounts (0 μL, 250 μL, 750 μL, and 1500 μL) of ^{15}N-*L*-Ile (30 mg·mL^{-1}) were added to the medium respectively and the strain were fermented for further 6 d. After the fermentation, the crudes were detected by LC-MS. Surprisingly, with the increase of the concentration of ^{15}N-*L*-Ile, the intensity of the $[M+H]^+$ ion at *m/z* 323 (corresponding to the ^{15}N-labeled isotopologue of compound **1**) also increased (Figure 5), which fully demonstrated that the 4-*oxo*-isoleucine portion of bipolamide C was derived from *L*-Ile.

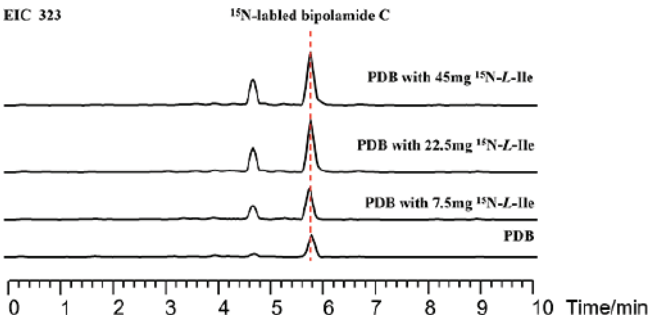

Figure 5 The $[M+H]^+$ ion fragment in the LC-MS of ^{15}N-labled compound **1** with different amounts of ^{15}N-*L*-Ile feeding extracts.

3.5 Proposed biosynthetic pathway of bipolamide C

To investigate the activation of the twn gene cluster by TwnD overexpression and the function of the oxidoreductase TwnB, we constructed individual knockout mutants of TwnA and TwnB in an *OE::TwnD* background. Specifically, the twnA knockout was created to verify cluster activation, while the twnB knockout was generated to determine its own enzymatic function. The results from the gene knockout experiments provided two key insights (Figure 6). First, the production of bipolamide C (**1**) was completely

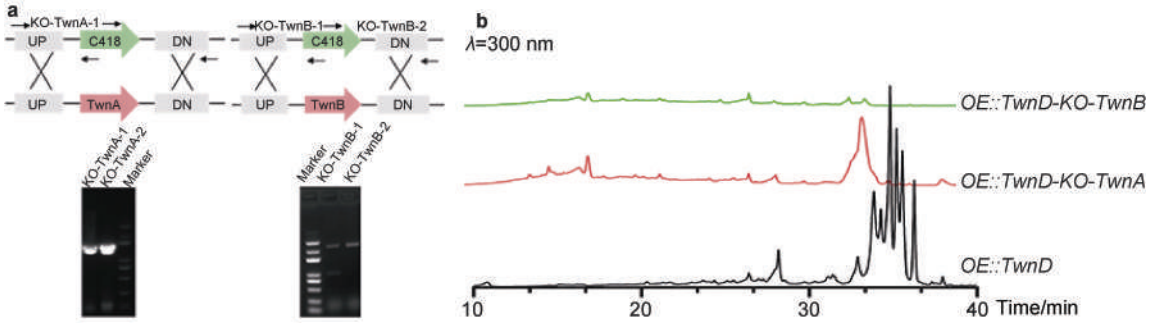

Figure 6 Knockout of TwnA or TwnB leads to the disappearance of compound **1**. **a**, PCR verification for TwnA or TwnB gene deletion. The black arrows represent the primer positions used for validation. **b**, HPLC analysis of the crude extracts from the *OE::TwnD-KO-TwnA*, *OE::TwnD-KO-TwnB* and the *OE::TwnD* mutants in PDB medium.

abolished in both the *OE::TwnD-KO-TwnA* and *OE::TwnD-KO-TwnB* strains. This genetically confirms that the biosynthesis of compound **1** is dependent on the *twn* gene cluster. Second, the essential role of TwnB suggests that the oxidative step it catalyzes (likely the conversion of *L*-Ile to 4-*oxo*-isoleucine) is a prerequisite for, or occurs concurrently with, the assembly steps carried out by TwnA and TwnE. This type of early oxidative tailoring is analogous to the functions of HtyE in echinocandin biosynthesis and RumG in rumbrin biosynthesis (Hüttel et al., 2016; Zhong et al., 2022).

Based on above results, we hypothesized that the biosynthetic process of bipolamide C involves the synergistic action of TwnA, TwnE and TwnB. Among them, TwnA and TwnE are responsible for catalyzing the processing of polyketide chain as well as the integration of 4-*oxo*-isoleucine, while the TwnB may be involved in the oxidation of isoleucine to generate 4-*oxo*-isoleucine. The detailed biosynthetic pathway speculation is shown in Figure 7.

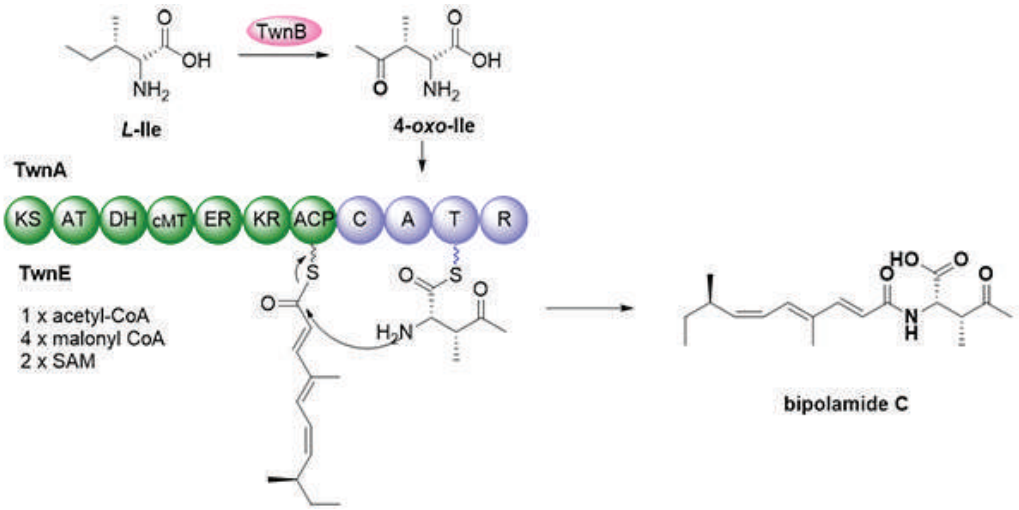

Figure 7 Proposed biosynthetic pathway of compound **1**.

4 Conclusion

In this study, the previously uncharacterized *twn* BGC in the Antarctic-derived fungus *Talaromyces* sp. HDN1820200 has been actived by overexpressing the pathway-specific transcriptional regulator TwnD. This led the production of one novel PKAA conjugate, bipolamide C (**1**) and one new polyketide variotin A (**2**). Bipolamide C features a 4-*oxo*-isoleucine moiety acylated with a polyketide-derived fatty acid, while variotin A exhibits a distinct unsaturated polyketide backbone. Feeding experiments confirmed that the unique 4-*oxo*-isoleucine unit in compound **1** originates from the oxidation of *L*-isoleucine. Gene knockout studies further demonstrated the essential roles of TwnA (PKS-NRPS) and TwnB in the biosynthesis of bipolamide C, supporting a proposed pathway involving iterative polyketide chain assembly, amino acid conjugation, and oxidative tailoring.

This work underscores the effectiveness of transcriptional factor overexpression as a strategy to unlock silent fungal biosynthetic pathways, particularly in extremophilic species. The discovery of bipolamide C and variotin A expands the chemical diversity of PKAA hybrids and highlights the untapped potential of specialized habitat-derived fungi for natural product discovery. Future studies could explore the biological activities of these compounds and further elucidate the enzymatic mechanisms within the *twn* cluster, providing insights into the evolution and functional versatility of fungal PKS-NRPS systems.

Acknowledgements This work was supported by the National Key R&D Program of China (Grant no. 2022YFC2807502), Qingdao Marine Science and Technology Center (Grant no. 2022QNLM030003-1) and Taishan Scholar Distinguished Expert Program in Shandong Province (Grant no. tstp20240504).

References

Blin K, Shaw S, Augustijn H E, et al. 2023. antiSMASH 7.0: new and improved predictions for detection, regulation, chemical structures and visualisation. Nucleic Acids Res, 51(W1): W46-W50, doi:10.1093/nar/gkad344.

Console-Bram L, Ciuciu S M, Zhao P W, et al. 2017. N-arachidonoyl glycine, another endogenous agonist of GPR55. Biochem Biophys Res Commun, 490(4): 1389-1393, doi:10.1016/j.bbrc.2017.07.038.

Gao Y L, Zhang M L, Wang X, et al. 2021. Isolation and characterization of a new cytotoxic polyketide-amino acid hybrid from *Thermothelomyces thermophilus* ATCC 42464. Nat Prod Res, 35(11): 1792-1798, doi:10.1080/14786419.2019.1641810.

Gilchrist C L M, Chooi Y H. 2021. Clinker & clustermap.js: automatic generation of gene cluster comparison figures. Bioinformatics, 37(16): 2473-2475, doi:10.1093/bioinformatics/btab007.

Grabiec U, Hohmann T, Ghadban C, et al. 2019. Protective effect of N-arachidonoyl glycine-GPR18 signaling after excitotoxical lesion in murine organotypic hippocampal slice cultures. Int J Mol Sci, 20(6):

1266, doi:10.3390/ijms20061266.

Hai Y, Tang Y. 2018. Biosynthesis of long-chain N-acyl amide by a truncated polyketide synthase-nonribosomal peptide synthetase hybrid megasynthase in fungi. J Am Chem Soc, 140(4): 1271-1274, doi:10.1021/jacs.7b13350.

Hüttel W, Youssar L, Grüning B A, et al. 2016. Echinocandin B biosynthesis: a biosynthetic cluster from *Aspergillus nidulans* NRRL 8112 and reassembly of the subclusters Ecd and Hty from *Aspergillus pachycristatus* NRRL 11440 reveals a single coherent gene cluster. BMC Genomics, 17: 570, doi:10.1186/s12864-016-2885-x.

Keating T A, Marshall C G, Walsh C T, et al. 2002. The structure of VibH represents nonribosomal peptide synthetase condensation, cyclization and epimerization domains. Nat Struct Biol, 9(7): 522-526, doi:10.1038/nsb810.

Kudo F. 2024. Biosynthesis of macrolactam antibiotics with β-amino acid polyketide starter units. J Antibiot, 77(8): 486-498, doi:10.1038/s41429-024-00742-2.

Kumar S, Stecher G, Li M, et al. 2018. MEGA X: molecular evolutionary genetics analysis across computing platforms. Mol Biol Evol, 35(6): 1547-1549, doi:10.1093/molbev/msy096.

Li H, Gilchrist C L M, Lacey H J, et al. 2019. Discovery and heterologous biosynthesis of the burnettramic acids: rare PKS-NRPS-derived bolaamphiphilic pyrrolizidinediones from an Australian fungus, *Aspergillus burnettii*. Org Lett, 21(5): 1287-1291, doi:10.1021/acs.orglett.8b04042.

Liu Z H, Friesen T L. 2012. Polyethylene glycol (PEG)-mediated transformation in filamentous fungal pathogens. Plant Fungal Pathogens. Totowa, NJ: Humana Press: 365-375, doi:10.1007/978-1-61779-501-5_21.

Morán M C, Pinazo A, Pérez L, et al. 2004. “Green” amino acid-based surfactants. Green Chem, 6(5): 233-240, doi:10.1039/B400293H.

Quevillon E, Silventoinen V, Pillai S, et al. 2005. InterProScan: protein domains identifier. Nucleic Acids Res, 33(Web Server issue): W116-W120, doi:10.1093/nar/gki442.

Rutledge P J, Challis G L. 2015. Discovery of microbial natural products by activation of silent biosynthetic gene clusters. Nat Rev Microbiol, 13(8): 509-523, doi:10.1038/nrmicro3496.

Scherlach K, Hertweck C. 2021. Mining and unearthing hidden biosynthetic potential. Nat Commun, 12: 3864, doi:10.1038/s41467-021-24133-5.

Seshadri K, Abad A N D, Nagasawa K K, et al. 2025. Synthetic biology in natural product biosynthesis. Chem Rev, 125(7): 3814-3931, doi:10.1021/acs.chemrev.4c00567.

Shu W S, Huang L N. 2022. Microbial diversity in extreme environments. Nat Rev Microbiol, 20(4): 219-235, doi:10.1038/s41579-021-00648-y.

Siriwach R, Kinoshita H, Kitani S, et al. 2014. Bipolamides A and B, triene amides isolated from the endophytic fungus *Bipolaris* sp. MU34. J Antibiot, 67(2): 167-170, doi:10.1038/ja.2013.103.

Wauchope H S, Shaw J D, Terauds A. 2019. A snapshot of biodiversity protection in Antarctica. Nat Commun, 10: 946, doi:10.1038/s41467-019-08915-6.

Yee D A, Tang Y. 2022. Investigating fungal biosynthetic pathways using heterologous gene expression: *Aspergillus nidulans* as a heterologous host. Methods Mol Biol, 2489: 41-52, doi:10.1007/978-1-0716-2273-5_3.

Zhang J M, Wang H H, Liu X, et al. 2020. Heterologous and engineered biosynthesis of nematocidal polyketide-nonribosomal peptide hybrid macrolactone from extreme thermophilic fungi. J Am Chem Soc, 142(4): 1957-1965, doi:10.1021/jacs.9b11410.

Zhong B F, Wan J, Shang C H, et al. 2022. Biosynthesis of rumbrins and inspiration for discovery of HIV inhibitors. Acta Pharm Sin B, 12(11): 4193-4203, doi:10.1016/j.apsb.2022.02.005.